Eur. Phys. J. A **30**, 579–589 (2006)
DOI 10.1140/epja/i2006-10145-2

THE EUROPEAN PHYSICAL JOURNAL A

Ternary fission within statistical approach

A.V. Andreev[1,2], G.G. Adamian[1,3,a], N.V. Antonenko[1,2], S.P. Ivanova[1], S.N. Kuklin[1], and W. Scheid[2]

[1] Joint Institute for Nuclear Research, 141980 Dubna, Russia
[2] Institut für Theoretische Physik der Justus-Liebig-Universität, D-35392 Giessen, Germany
[3] Institute of Nuclear Physics, Tashkent 702132, Uzbekistan

Received: 20 March 2006 / Revised: 6 November 2006 /
Published online: 5 December 2006 –
Communicated by D. Guerreau

Abstract. The ternary system with a light nucleus between two heavy fragments is assumed to appear from the binary configuration near scission. The formation of a third light nucleus in the binary system is considered. The calculated charge distributions in spontaneous ternary fission of ^{252}Cf and in induced ternary fission of ^{56}Ni are compared with the available experimental data. The neutron multiplicity from the fission fragments is described. The fine structures of the TKE-mass distribution are predicted.

PACS. 25.85.-w Fission reactions – 21.60.Gx Cluster models

1 Introduction

In the last two decades there were many experiments [1–6] carried out on the spontaneous ternary fission of ^{252}Cf which is convenient for measurements. Recently, interesting preliminary results on the induced ternary fission of ^{56}Ni were obtained by von Oertzen *et al.* [7]. The study of these rare processes is a challenge for the theory and is important for the understanding of the fission mechanism. Due to the emission of a light charged particle (LCP) from the region between the two heavy fragments, the process of formation of fission fragments near the scission becomes observable and the nuclear shape at scission can be explored. Based on the experimental information it has been suggested in ref. [8] that the ternary fission is a particular case of binary fission, *i.e.* the LCP is formed in the process of binary fission. The microscopic study [9] of the formation probability of an α-particle in the fissioning nucleus supports the formation of an α-particle between the heavy fragments in the last stage of the fission process. The same conclusion follows from the classical and semiclassical dynamical and statistical treatments [10–13].

In the present paper we will also assume that the ternary fission is a two-step process. In the first step the binary system is formed, in the second step the third light nucleus originates from one or several alpha particles and neutrons in the region between the two separating heavy fragments. This mechanism will be supported by our calculations of such characteristics of ternary fission as the charge distribution, total kinetic energy (TKE) of the fission fragments, and neutron multiplicity distribution from the fission fragments. We will use the statistical approach based on the potential energies of the ternary systems with certain LCP. A similar model was used by us in ref. [14] for the description of binary fission. As shown in ref. [12], the statistical approach is suitable to describe the relative yields of various ternary decays.

In sect. 2 the methods of calculation of the potential energy of the ternary system at scission and the charge distributions in ternary fission will be described. The potential energies of various ternary systems as functions of deformations of heavy fragments will be analysed. We will define the most probable deformations of the fragments at scission. The TKE of fission fragments will be defined as the interaction potential at scission which depends strongly on the deformations of the fragments. The excitation energies of the fragments after spontaneous ternary fission and neutron multiplicity from these fragments will be studied. In sect. 3 the results of our calculations for ^{252}Cf and ^{58}Ni will be discussed.

2 Model

2.1 Potential energy of the ternary system

Considering the ternary fission as a two-step process, we assume the formation of the LCP between the heavy fragments after the formation of the scission configuration of the binary system. The treated ternary system at scission consists of three almost touching coaxial ellipsoids: two heavy fragments 1 and 2, and the light fragment 3 between them (see fig. 1). Note that in this system the LCP

[a] e-mail: adamian@theor.jinr.ru

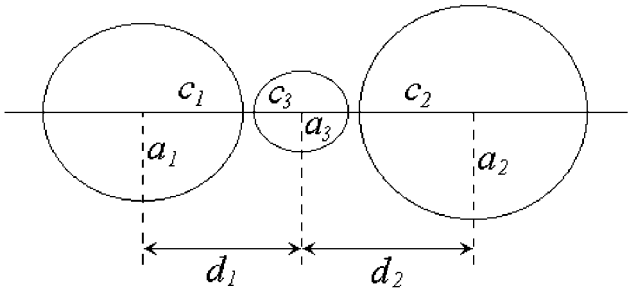

Fig. 1. Scission configuration of the ternary system.

can have the kinetic energy which is the subject of future dynamical calculations. The main parameters describing the ternary system are the charges (Z_i) and the masses (A_i) of the fragments, the distances between the centers of the fragments (d_1 and d_2), the deformation parameters (β_i), and the excitation energy of the whole system E^*. The deformation parameters β_i are defined as the ratios of the major (c_i) and minor (a_i) semiaxes of the ellipsoids $\beta_i = c_i/a_i$. The volume conservation is taken into account. The potential energy of the ternary system $(Z_1, A_1) + (Z_3, A_3) + (Z_2, A_2)$ is defined as follows:

$$U(\{A_i, Z_i, \beta_i, d_i\}, E^*) = U_1^{LD}(A_1, Z_1, \beta_1) + U_2^{LD}(A_2, Z_2, \beta_2) + \delta U_1^{sh}(A_1, Z_1, \beta_1, E^*) + \delta U_2^{sh}(A_2, Z_2, \beta_2, E^*) + U_3(A_3, Z_3) + V_{int}(\{A_i, Z_i, \beta_i, d_i\}, L) \quad (1)$$

with

$$V_{int}(\{A_i, Z_i, \beta_i, d_i\}, L) = V_{12}^C(A_1, Z_1, A_2, Z_2, \beta_1, \beta_2, d_1+d_2) + V_{12}^N(A_1, A_2, \beta_1, \beta_2, d_1+d_2) + V_{13}^C(A_1, Z_1, A_3, Z_3, \beta_1, \beta_3, d_1) + V_{13}^N(A_1, A_3, \beta_1, \beta_3, d_1) + V_{23}^C(A_2, Z_2, A_3, Z_3, \beta_2, \beta_3, d_2) + V_{23}^N(A_2, A_3, \beta_2, \beta_3, d_2) + V^{rot}(\{A_i, \beta_i, d_i\}).$$

The potential energies of the heavy fragments consist of the liquid-drop energies U_i^{LD} and shell correction δU_i^{sh} terms which depend on the deformations of the fragments. The values of U_1^{LD} and U_2^{LD} are calculated like in ref. [14] where the method of calculation of δU_i^{sh} with the two-center shell model [15] is described as well. Since we consider only a light third fragment up to oxygen, this fragment is stiff and its potential energy U_3 was taken at fixed deformation of the ground state. The interaction potential V_{int} contains three Coulomb V_{ij}^C and nuclear V_{ij}^N interactions between the fragments. The calculation of V_{ij}^N is done in the double-folding procedure with Skyrme-type density-dependent nucleon-nucleon forces [16,17]. The diffuseness parameters for the Fermi distribution of the nucleon densities are 0.48, 0.52 and 0.55 fm for ^{4}He, ^{8,10}Be and other nuclei, respectively. The parameters of radii of ^{4}He, ^{8,10}Be and other nuclei are 1.03, 1.12 and 1.15 fm, respectively. If the compound nucleus is obtained in the reaction like $^{32}\mathrm{S} + {}^{24}\mathrm{Mg} \rightarrow {}^{56}\mathrm{Ni}$ and has large angular momentum, then we take into consideration the rotational energy term $V^{rot} = \hbar^2 L(L+1)/(2\Im)$ with the rigid-body moment of inertia $\Im$. For spontaneous ternary fission of ^{252}Cf, we set $V^{rot} = 0$.

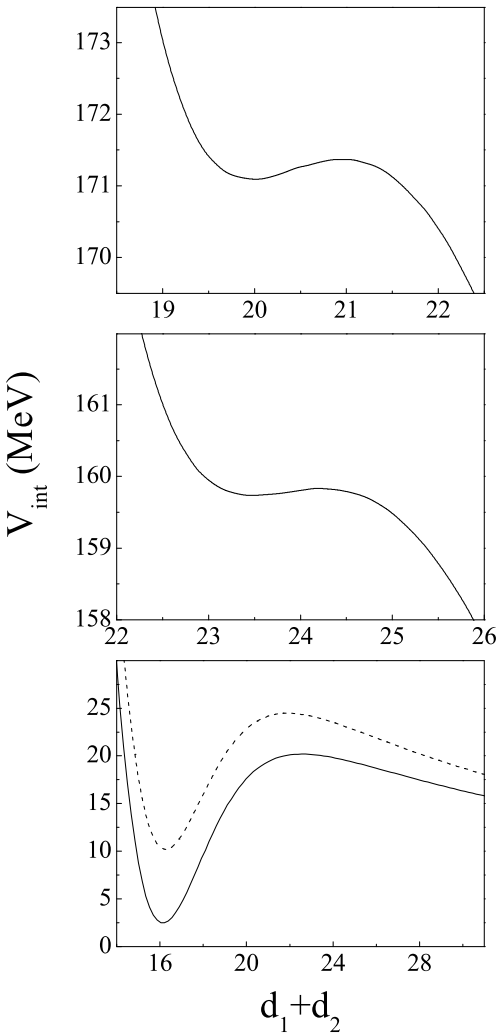

Fig. 2. Calculated interaction potentials for the ternary systems $^{106}\mathrm{Mo} + {}^4\mathrm{He} + {}^{142}\mathrm{Xe}$ (upper part) and $^{102}\mathrm{Zr} + {}^{10}\mathrm{Be} + {}^{140}\mathrm{Xe}$ (middle part) at $L = 0$, and for $^{20}\mathrm{Ne} + {}^8\mathrm{Be} + {}^{28}\mathrm{Si}$ (lower part) at $L = 0$ (solid line) and $L = 35$ (dashed line) as a function of the distance between the heavy fragments, $d_1 + d_2$. The condition $A_1 d_1 = A_2 d_2$ is used. The deformations of heavy fragments correspond to the deepest minimum of the potential energy as a function of β_1 and β_2.

For particular ternary systems with some deformations, the interaction potential V_{int} as a function of the distances d_1 and d_2 has a potential barrier which results from the competition between the repulsive Coulomb and attractive nuclear interactions. In the spontaneous fission of ^{252}Cf it is about 0.5 MeV, in the induced fission of ^{56}Ni this barrier is more than 10 MeV. For the calculation of the relative yields we should use the values of potential energy on the barrier at $R_b = d_1 + d_2$ which depends on the choice of the relationship between d_1 and d_2. For the fission of actinides, this choice weakly influences the results because the barrier remains small for each ratio between d_1 and

d_2. The experiment [7] for induced ternary fission of ^{56}Ni with third particles ^{8}Be and ^{12}C demonstrates a very narrow distribution of the out-of-plane angle between the first and the second fragments near 180°, hence, the third particle has approximately zero velocity in the center-of-mass coordinate system. Using this fact, we set $A_1 d_1 = A_2 d_2$ [8, 18] and take for the potential energy calculation the values of d_1 and d_2 corresponding to the barrier along this path. The results for the systems $^{106}\mathrm{Mo} + {}^{4}\mathrm{He} + {}^{142}\mathrm{Xe}$, $^{102}\mathrm{Zr} + {}^{10}\mathrm{Be} + {}^{140}\mathrm{Xe}$ and $^{20}\mathrm{Ne} + {}^{8}\mathrm{Be} + {}^{28}\mathrm{Si}$ are presented in fig. 2. While the ternary systems formed from ^{252}Cf are unstable with respect to decay, the decay of the ternary systems formed from ^{56}Ni demands considerable energy. As one can see, the treated ternary systems can be called the scission configurations because they either are kept by small potential barriers or correspond to the minimal repulsive forces (the Coulomb repulsion is almost compensated by the nuclear attraction). In our opinion this fact allows us to assume some thermal equilibrium and to use the statistical treatment.

The intrinsic excitation energy of the scission configuration is related to the Q-value as follows:

$$E^*(\{A_i, Z_i, \beta_i\}, R_b) = Q - \sum_{i \neq j} (V_{ij}^C + V_{ij}^N) + \delta V^{rot} - E_{def}(\{A_i, Z_i, \beta_i\}) + S, \quad (2)$$

where E_{def} is the deformation energy arising from the deviation of β_i from the values corresponding to the nuclear ground states; S is the excitation energy of the fissioning nucleus, and δV^{rot} the change of rotational energy of the scission configuration with respect to the compound nucleus. In spontaneous fission $S = 0$ and $\delta V^{rot} = 0$. The dynamics of the ternary fission is not treated here. We only consider effects which can be explained with the statistical approach. Therefore, in eq. (2) we assume that the energy related to the motion and internal excitation of the LCP in the field of the two heavy fragments at the scission configuration is equal to zero. We also disregard the kinetic energy of the heavy fragments at scission.

In order to include the dependence of the shell correction on the excitation energy E^*, the following phenomenological expression is widely used:

$$\delta U_i^{sh}(A_i, Z_i, \beta_i, E^*) = \delta U_i^{sh}(A_i, Z_i, \beta_i, E^* = 0) \exp[-E_i^*/E_D], \quad (3)$$

where the excitation energy is divided between the heavy fragments proportional to their level density parameters a_i, *i.e.* $E_i^* = a_i E^*/(a_1 + a_2)$. The damping constant E_D is set as 18.5 MeV [19]. We found for the considered excitation energies that our final results are not very sensitive to a reasonable variation of E_D within the interval 15–25 MeV. The level density is calculated with the parameter [19]

$$a_i = \tilde{a}_i(A_i) \left[1 + \frac{1 - \exp\{-(E - E_c)/E_D\}}{E - E_c} \delta U_i^{sh}\right], \quad (4)$$

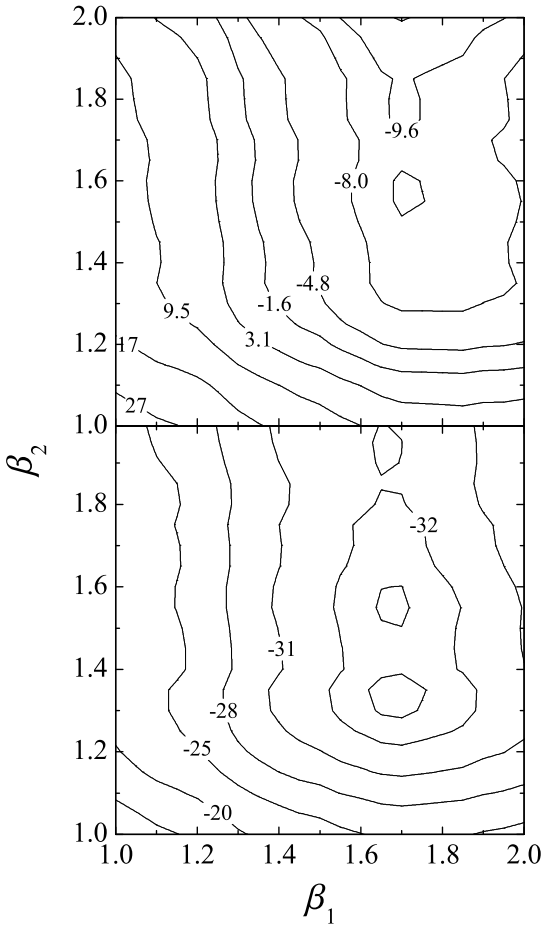

Fig. 3. Potential energy surfaces for the binary system $^{106}\mathrm{Mo} + {}^{146}\mathrm{Ba}$ (upper part) and the ternary system $^{106}\mathrm{Mo} + {}^{4}\mathrm{He} + {}^{142}\mathrm{Xe}$ (lower part). The energies are given in MeV with respect to the ground state of ^{252}Cf. The calculations are performed with the method and parameters indicated in refs. [14,15].

where we take the parameter $\tilde{a}_i(A_i)$ proportional to A_i, and E_c is the energy of condensation which reduces the ground-state energy of a Fermi gas by 2 MeV.

Since the potential energy depends on E^*, the excitation energy is calculated with (2) by using an iteration procedure. First, U in eq. (1) is defined with $E^* = 0$ MeV and a new value of E^* is found from (2). Then, with this E^* we calculate the potential energy U which leads to a new value of E^*. As we checked, these two steps supply a nice accuracy in finding E^*.

In the fission of a heavy nucleus the heavy fragments in a ternary system can be significantly deformed under the influence of each other. To find the equilibrium deformations of the fragments at scission for each mass and charge splitting, we calculate the potential energy surface as a function of deformations of the heavy fragments. Due to the shell effects, there can be one or several shallow minima on the potential energy surface. Within the statistical approach one can conclude that the ternary system decays with relatively large probabilities from configurations with

deformations corresponding to these minima [14]. Analogously to binary fission, the enhanced yields from the shallow potential minima can create the fine structure in the TKE-mass distribution [14]. Since in the ternary configurations considered the distance between the heavy fragments is larger than in the binary case, the Coulomb interaction is smaller and the mutual influence of the fragments is weaker. Hence, the deformations in the deepest minimum are smaller in ternary systems. Figure 3 demonstrates the example of the potential energy surface for a ternary system in comparison with a binary system. If one of the fragments is a magic nucleus, its deformation in the minimum weakly deviates from the deformation of the ground state. For a non-magic fragment, the minimum corresponds to a quite large deformation of this fragment.

2.2 Ternary fission as a two-step process

Our calculations show that the potential energies of ternary systems in actinides are about 20 MeV smaller than in binary systems. If we assume a straight formation of the ternary system which competes with the formation of the binary system, then the ternary fission would have a larger yield than the binary fission. Since this contradicts the experimental results, the ternary system is not straightly formed. The binary system is firstly formed and then the ternary system is formed from it by extracting the LCP into the region between the two heavy fragments. Then this ternary system decays. In this picture the charge distribution for ternary fission is strongly ruled by the one for the binary fission. Such relationships between the binary and ternary charge distributions really exist in the experiment [2].

There is more compact ternary configuration between the binary scission configuration (first step of the model) and the ternary scission configuration (second step). While in this compact ternary configuration the potential energy of the LCP is maximal on the symmetry axis and decreases with the deviation of the LCP in the perpendicular direction (in the coordinate ρ), in the ternary scission configuration the position of the LCP on the symmetry axis corresponds to the conditional minimum of the potential. Due to the drastic change of the potential for the LCP, the LCP can obtain the valuable kinetic energy when the system moves from the compact ternary configuration to the ternary scission configuration considered. Indeed, in the compact ternary configuration the LCP is accelerated in the perpendicular direction (in ρ). The preliminary dynamical calculations result the small, about 2 MeV, kinetic energy of the heavy fragments and the kinetic energy of the LCP of about 15 MeV at the ternary scission configuration considered. Since the dynamics of the ternary fission is not treated here, the kinetic energies of the LCP and heavy fragments at scission are disregarded in our calculations. This leads to an overestimation of E^* in eq. (2) and, thus, of the width of the charge and mass distributions.

Since the ternary scission configuration is in the conditional potential minimum in R and in ρ, the application of the statistical approach is justified. Using the statistical approach, one can estimate the relative yields of ternary systems with a given LCP (Z_3, A_3). First, the relative probability for the formation of the binary system containing the fragments (Z_1^b, A_1^b) and (Z_2^b, A_2^b) is calculated as follows:

$$Y_b(A_1^b, Z_1^b) = Y_b^0 \iint \exp(-U_b(A_1^b, Z_1^b, \beta_1, A_2^b, Z_2^b, \beta_2, E^*)/T) \mathrm{d}\beta_1 \mathrm{d}\beta_2, \quad (5)$$

where Y_b^0 is the normalization factor. The sums $A_1^b + A_2^b$ and $Z_1^b + Z_2^b$ are equal to the mass and charge numbers of the fissioning nucleus, respectively. The potential energy U_b of the binary system for each pair of deformations β_1 and β_2 is taken in the minimum of the interaction potential at $R_m \approx c_1 + c_2 + 0.5\,\mathrm{fm}$. Here, $T = (E^*/a)^{1/2}$ ($a = A/12\,\mathrm{MeV}^{-1}$) is the temperature corresponding to E^* of that binary system which has the minimal potential energy among the systems considered. Then, from each binary system several ternary systems with different charge asymmetries can be formed by extracting one or several α-particles and several neutrons from one or both fragments. Different variants of the formation of the ternary system from the binary one are listed in table 1 for ^{252}Cf and in table 2 for ^{56}Ni. For each binary system and certain LCP, the relative probabilities for the ternary systems are calculated as follows:

$$Y_t(Z_1, A_1, Z_3, A_3, Z_1^b, A_1^b) = Y_t^0(Z_3, A_3, Z_1^b, A_1^b) \times \iint \exp(-U(A_1, Z_1, \beta_1, A_2, Z_2, \beta_2, A_3, Z_3, E^*)/T) \mathrm{d}\beta_1 \mathrm{d}\beta_2, \quad (6)$$

where $Y_t^0(Z_3, A_3, Z_1^b, A_1^b)$ is the normalization factor and the potential energies correspond to the barriers at R_b depending on β_i. The sums $A_1 + A_2 + A_3$ and $Z_1 + Z_2 + Z_3$ are equal to the mass and charge numbers of the fissioning nucleus, respectively. To find the yield of decay of a certain ternary system formed from a certain binary system, we multiply the corresponding probabilities: $Y_b(Z_1^b, A_1^b) Y_t(Z_1, A_1, Z_3, A_3, Z_1^b, A_1^b)$. Finally, we sum the yields for the systems with the same charge asymmetries and the same LCP and obtain the primary charge distribution:

$$Y(Z_1, Z_3, A_3) = \sum_{Z_1^b, A_1^b, A_1} Y_b(Z_1^b, A_1^b) Y_t(Z_1, A_1, Z_3, Z_1^b, A_1^b). \quad (7)$$

It is clear from the method used that the obtained charge distribution Y is normalized to unity. In order to simplify the calculations, for each set (Z_1, Z_1^b, A_1^b) in eq. (7) we take the most probable A_1. Using the idea that the ternary system is formed in the second step after the formation of the binary system, the relative yields of various ternary systems with the same LCP will be calculated.

Table 1. Calculated relative probabilities for the formation of ternary systems from the indicated binary systems in the ^{4}He- and ^{10}Be-accompanied spontaneous ternary fission of ^{252}Cf. The sum of all presented values of Y_b is equal to unity. For each binary system, the sum of Y_t is normalized to unity.

Binary system	Y_b	Ternary system	Y_t	Y_bY_t	Ternary system	Y_t	Y_bY_t
^{96}Sr + ^{156}Nd	0.025	^{92}Kr + ^{4}He + ^{156}Nd	0.22	0.0055	^{86}Se + ^{10}Be + ^{156}Nd	0.04	0.001
		^{96}Sr + ^{4}He + ^{152}Ce	0.78	0.0195	^{92}Kr + ^{10}Be + ^{150}Ce	0.36	0.009
					^{96}Sr + ^{10}Be + ^{146}Ba	0.6	0.015
^{98}Sr + ^{154}Nd	0.04	^{94}Kr + ^{4}He + ^{154}Nd	0.13	0.005	^{88}Se + ^{10}Be + ^{154}Nd	0.03	0.0012
		^{98}Sr + ^{4}He + ^{150}Ce	0.87	0.035	^{92}Kr + ^{10}Be + ^{150}Ce	0.27	0.011
					^{98}Sr + ^{10}Be + ^{144}Ba	0.7	0.028
^{100}Sr + ^{152}Nd	0.01	^{96}Kr + ^{4}He + ^{152}Nd	0.04	0.0004	^{90}Se + ^{10}Be + ^{152}Nd	0.02	0.0002
		^{100}Sr + ^{4}He + ^{148}Ce	0.96	0.0096	^{94}Kr + ^{10}Be + ^{148}Ce	0.25	0.0025
					^{100}Sr + ^{10}Be + ^{142}Ba	0.73	0.0073
^{100}Zr + ^{152}Ce	0.023	^{96}Sr + ^{4}He + ^{152}Ce	0.56	0.013	^{90}Kr + ^{10}Be + ^{152}Ce	0.05	0.0012
		^{100}Zr + ^{4}He + ^{148}Ba	0.44	0.01	^{96}Sr + ^{10}Be + ^{146}Ba	0.36	0.0083
					^{100}Zr + ^{10}Be + ^{142}Xe	0.59	0.014
^{102}Zr + ^{150}Ce	0.11	^{98}Sr + ^{4}He + ^{150}Ce	0.36	0.04	^{92}Kr + ^{10}Be + ^{150}Ce	0.09	0.01
		^{102}Zr + ^{4}He + ^{146}Ba	0.64	0.07	^{98}Sr + ^{10}Be + ^{144}Ba	0.22	0.024
					^{102}Zr + ^{10}Be + ^{140}Xe	0.69	0.076
^{104}Zr + ^{148}Ce	0.05	^{100}Sr + ^{4}He + ^{148}Ce	0.21	0.01	^{94}Kr + ^{10}Be + ^{148}Ce	0.04	0.002
		^{104}Zr + ^{4}He + ^{144}Ba	0.79	0.04	^{98}Sr + ^{10}Be + ^{144}Ba	0.37	0.018
					^{104}Zr + ^{10}Be + ^{138}Xe	0.59	0.03
^{104}Mo + ^{148}Ba	0.017	^{100}Zr + ^{4}He + ^{148}Ba	0.56	0.0095	^{94}Sr + ^{10}Be + ^{148}Ba	0.07	0.0012
		^{104}Mo + ^{4}He + ^{144}Xe	0.44	0.0075	^{100}Zr + ^{10}Be + ^{142}Xe	0.6	0.01
					^{104}Mo + ^{10}Be + ^{138}Te	0.33	0.0056
^{106}Mo + ^{146}Ba	0.2	^{102}Zr + ^{4}He + ^{146}Ba	0.41	0.08	^{96}Sr + ^{10}Be + ^{146}Ba	0.1	0.02
		^{106}Mo + ^{4}He + ^{142}Xe	0.59	0.12	^{102}Zr + ^{10}Be + ^{140}Xe	0.48	0.096
					^{106}Mo + ^{10}Be + ^{136}Te	0.42	0.084
^{108}Mo + ^{144}Ba	0.17	^{104}Zr + ^{4}He + ^{144}Ba	0.4	0.068	^{98}Sr + ^{10}Be + ^{144}Ba	0.11	0.019
		^{108}Mo + ^{4}He + ^{140}Xe	0.6	0.102	^{102}Zr + ^{10}Be + ^{140}Xe	0.35	0.06
					^{108}Mo + ^{10}Be + ^{134}Te	0.54	0.09
^{110}Mo + ^{142}Ba	0.05	^{104}Zr + ^{4}He + ^{144}Ba	0.2	0.01	^{100}Sr + ^{10}Be + ^{142}Ba	0.08	0.004
		^{108}Mo + ^{4}He + ^{140}Xe	0.8	0.04	^{104}Zr + ^{10}Be + ^{138}Xe	0.36	0.018
					^{110}Mo + ^{10}Be + ^{132}Te	0.56	0.028
^{110}Ru + ^{142}Xe	0.043	^{106}Mo + ^{4}He + ^{142}Xe	0.73	0.031	^{100}Zr + ^{10}Be + ^{142}Xe	0.21	0.009
		^{110}Ru + ^{4}He + ^{138}Te	0.27	0.012	^{106}Mo + ^{10}Be + ^{136}Te	0.53	0.023
					^{110}Ru + ^{10}Be + ^{132}Sn	0.26	0.011
^{112}Ru + ^{140}Xe	0.14	^{108}Mo + ^{4}He + ^{140}Xe	0.31	0.043	^{102}Zr + ^{10}Be + ^{140}Xe	0.26	0.036
		^{112}Ru + ^{4}He + ^{136}Te	0.69	0.097	^{108}Mo + ^{10}Be + ^{134}Te	0.4	0.056
					^{112}Ru + ^{10}Be + ^{130}Sn	0.34	0.048
^{114}Ru + ^{138}Xe	0.055	^{110}Mo + ^{4}He + ^{138}Xe	0.35	0.019	^{104}Zr + ^{10}Be + ^{138}Xe	0.17	0.009
		^{114}Ru + ^{4}He + ^{134}Te	0.65	0.036	^{108}Mo + ^{10}Be + ^{134}Te	0.48	0.026
					^{114}Ru + ^{10}Be + ^{128}Sn	0.35	0.019
^{116}Pd + ^{136}Te	0.01	^{112}Ru + ^{4}He + ^{136}Te	0.91	0.0091	^{106}Mo + ^{10}Be + ^{136}Te	0.27	0.0027
		^{116}Pd + ^{4}He + ^{132}Sn	0.09	0.0009	^{112}Ru + ^{10}Be + ^{130}Sn	0.4	0.004
					^{116}Pd + ^{10}Be + ^{126}Cd	0.33	0.0033
^{118}Pd + ^{134}Te	0.027	^{114}Ru + ^{4}He + ^{134}Te	0.57	0.0154	^{108}Mo + ^{10}Be + ^{134}Te	0.3	0.008
		^{118}Pd + ^{4}He + ^{130}Sn	0.43	0.0116	^{112}Ru + ^{10}Be + ^{130}Sn	0.26	0.007
					^{118}Pd + ^{10}Be + ^{124}Cd	0.44	0.012
^{120}Pd + ^{132}Te	0.03	^{116}Ru + ^{4}He + ^{132}Te	0.47	0.014	^{110}Mo + ^{10}Be + ^{132}Te	0.24	0.0072
		^{120}Pd + ^{4}He + ^{128}Sn	0.53	0.016	^{114}Ru + ^{10}Be + ^{128}Sn	0.32	0.0096
					^{120}Pd + ^{10}Be + ^{122}Cd	0.44	0.013

Table 2. Calculated relative probabilities for the formation of ternary systems from the indicated binary systems in the ^{8}Be-accompanied ternary fission of ^{56}Ni. The sum of all presented values of Y_b is equal to unity. For each binary system, the sum of Y_t is normalized to unity.

Binary system	Y_b	Ternary system	Y_t	Y_bY_t
^{20}Ne + ^{36}Ar	0.19	^{16}O + ^{8}Be + ^{32}S	0.64	0.122
		^{20}Ne + ^{8}Be + ^{28}Si	0.36	0.068
^{22}Na + ^{34}Cl	0.02	^{18}F + ^{8}Be + ^{30}P	0.68	0.0136
		^{22}Na + ^{8}Be + ^{26}Al	0.32	0.0064
^{24}Mg + ^{32}S	0.25	^{16}O + ^{8}Be + ^{32}S	0.5	0.125
		^{20}Ne + ^{8}Be + ^{28}Si	0.28	0.07
		^{24}Mg + ^{8}Be + ^{24}Mg	0.22	0.055
^{26}Al + ^{30}P	0.03	^{18}F + ^{8}Be + ^{30}P	0.68	0.02
		^{26}Mg + ^{8}Be + ^{22}Na	0.32	0.01
^{28}Si + ^{28}Si	0.51	^{20}Ne + ^{8}Be + ^{28}Si	0.57	0.29
		^{24}Mg + ^{8}Be + ^{24}Mg	0.43	0.22

2.3 Relative yields of different LCP

It is also interesting to calculate the ratios of the yields of different LCP. The analysis of potential energy surfaces at scission does not provide this information. The relative yields of ternary fission with various LCP are determined by the formation probability S of LCP and the probability of ternary decay (the LCP can be absorbed by one of the fragments that leads to binary decay). To calculate the formation probability of LCP, we find the spectroscopic factors for different LCP within our cluster approach [20]. The spectroscopic factor is the weight of a certain binary cluster configuration in the wave function of the nucleus.

In the cluster model, the charge (mass) asymmetry coordinate $\eta_Z = (Z_d - Z_x)/(Z_d + Z_x)$ ($\eta = (A_d - A_x)/(A_d + A_x)$), which describes a partition of protons (nucleons) between the nuclei of the dinuclear system formed by two touching nuclei or clusters, is used as relevant collective variable. Here, Z_d (A_d) and Z_x (A_x) are the charge (mass) numbers of the heavy and light nuclei of the dinuclear system, respectively. In the dynamical treatment η (η_Z) is assumed as a continuous variable [20]. The wave function in η_Z can be thought as a superposition of the mononucleus configuration with $|\eta_Z| = |\eta| = 1$ and different cluster-type configurations including the most probable alpha-cluster configuration with $|\eta_Z| = 1 - 4/(Z_d + Z_x)$ ($Z_x = 2$). The relative weight of each cluster component in the total wave function is determined by solving the stationary Schrödinger equation

$$\left[-\frac{\hbar^2}{2}\frac{\mathrm{d}}{\mathrm{d}\eta_Z}B_{\eta_Z}^{-1}\frac{\mathrm{d}}{\mathrm{d}\eta_Z} + U_{dr}(\eta_Z)\right]\Psi_i(\eta_Z) = E_i\Psi_i(\eta_Z), \quad (8)$$

where $B_{\eta_Z}^{-1}$ and $U_{dr}(\eta_Z)$ are the inverse inertia coefficient and potential energy (driving potential) of the collective Hamiltonian in η_Z, respectively. A method of calculation of $B_{\eta_Z}^{-1}$ is described in ref. [20]. The potential $U_{dr}(\eta_Z)$ of cluster systems ($|\eta_Z| < 1$) is taken as

$$U_{dr}(\eta_Z) = V(R_m, \eta_Z) - B_d(\eta_Z) - B_x(\eta_Z) + B,$$
$$V(R_m, \eta_Z) = V^C(R_m, \eta_Z) + V^N(R_m, \eta_Z). \quad (9)$$

The quantities B_d and B_x are the experimental binding energies of the clusters forming the dinuclear system at a given η_Z, and B is the experimental binding energy of the mother nucleus. These values are taken from ref. [21]. Due to the normalization by B in eq. (9), $E_{i=0} = 0$ for the ground state. The nucleus-nucleus potential V is the sum of the nuclear V^N and the Coulomb V^C ones. Here, the nuclear rotation is not treated. The dinuclear system is localized in the minimum of the pocket of the nucleus-nucleus interaction potential V at the relative distance $R = R_m$ corresponding to the touching configuration. The deformations of the heavy cluster are taken from refs. [22, 23]. The pole-to-pole orientation of the deformed nuclei in the dinuclear system gives the minimum of the potential energy. Since the mode responsible for the N/Z equilibrium in the dinuclear system is quite fast, the potential energy U_{dr} is minimized with respect to η for each η_Z. The expression (9) cannot be used to calculate the potential energy of a mononucleus. With calculated $B_{\eta_Z}^{-1}$ the value of $U_{dr}(|\eta_Z| = |\eta| = 1)$ was chosen so to have $E_{i=0} = 0$ for the ground state.

Taking into consideration that the population probability of the state $\Psi_i(\eta_Z, I)$ in η_Z is proportional to $\exp(-E_i/T)$, the spectroscopic factor S_x of a cluster with Z_x is calculated as follows:

$$S_x = \sum_i \exp\left(-\frac{E_i}{T}\right) \times \int_{\eta_Z(Z_x)-1/Z}^{\eta_Z(Z_x)+1/Z} |\Psi_i(\eta_Z, I)|^2 \mathrm{d}\eta_Z / \sum_i \exp\left(-\frac{E_i}{T}\right). \quad (10)$$

Here, $0.5|\eta_Z(Z_x) - \eta_Z(Z_x \pm 1)| = 1/Z$ is the half-distance in units of η_Z between the dinuclear configurations with Z_x and $Z_x \pm 1$. In this approach the collective motion in the mass asymmetry coordinate simultaneously creates a deformation with even and odd multipolarities. So, the clusterization is strongly related to the excitation of quadrupole and octupole vibrations. Therefore, the cluster formation would increase with excitation en-

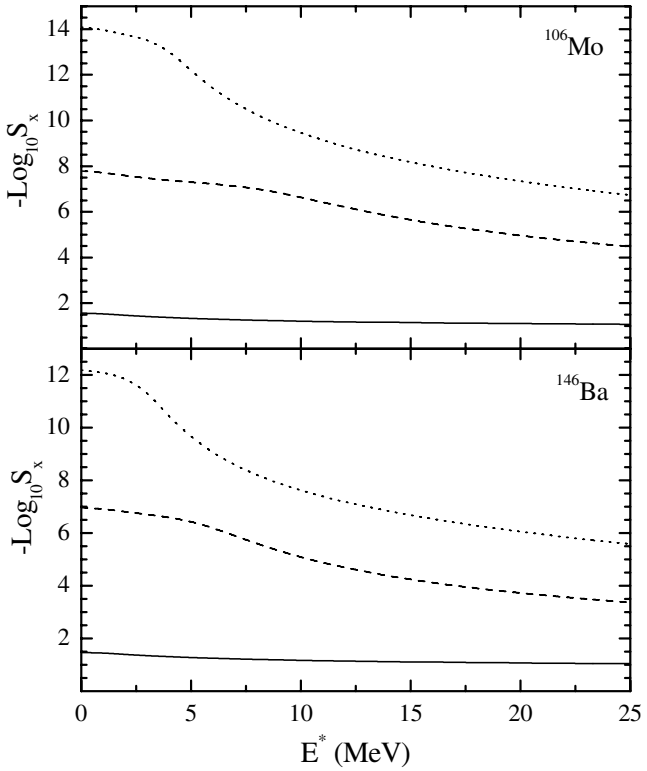

Fig. 4. Spectroscopic factors for ^{4}He (solid line), ^{10}Be (dashed line) and ^{14}C (dotted line) as functions of excitation energy in the nuclei ^{106}Mo (upper part) and ^{146}Ba (lower part).

ergy. For zero excitation, eq. (10) is transformed into $S_x = \int\limits_{\eta_Z(Z_x)-1/Z}^{\eta_Z(Z_x)+1/Z} |\Psi_0(\eta_Z)|^2 \mathrm{d}\eta_Z$ and leads to the values consistent with the results of ref. [24].

We calculate the spectroscopic factors S_x for different nuclei from Sr to Nd [25]. The spectroscopic factors for ^{4}He, ^{10}Be and ^{14}C in ^{106}Mo and ^{146}Ba are shown in fig. 4 as functions of excitation energy. The excitation energies of the fragments in binary systems formed from ^{252}Cf are about 10–15 MeV. In this case the spectroscopic factors for ^{4}He $S(^4\mathrm{He}) = S_{^4\mathrm{He}} = 5 \times 10^{-2}$ are found to be close to each other for all fragments considered. The spectroscopic factors for ^{10}Be for all these nuclei are at least two orders of magnitude smaller than the product $S(^{10}\mathrm{Be}) = S_{^4\mathrm{He}} \times S_{^4\mathrm{He}} = 2.5 \times 10^{-3}$. This means that the LCP ^{10}Be can be formed consequently by two α-particles and two neutrons between two heavy fragments. Since the formation of ^{4}He in the region between the heavy fragments is preferable, this region is marked out and one can assume that two sequentially formed ^{4}He are correlated to form ^{10}Be. The α-particles can be extracted from one or both fragments of the binary system. Two neutrons are easily absorbed by ^{8}Be because the configurations with ^{10}Be correspond to smaller potential energies. Then, we can suppose that the neutrons do not change the probability of formation. Analogously, the formation probabilities of ^{14}C and ^{20}O as LCP are $S(^{14}\mathrm{C}) = (S_{^4\mathrm{He}})^3$ and $S(^{20}\mathrm{O}) = (S_{^4\mathrm{He}})^4$, respectively.

Table 3. Correlation of the formation probabilities S and experimental relative yields Y_{exp} [1] of different LCP. The values of S and Y_{exp} are given with respect to those for ^{4}He.

LCP	$Y_{exp}/Y_{exp}(^4\mathrm{He})$	$S/S_{^4\mathrm{He}}$
^{4}He	1	1
^{7}Li	5×10^{-3}	4.2×10^{-3}
^{10}Be	1.3×10^{-2}	5×10^{-2}
^{11}B	6×10^{-4}	2.1×10^{-4}
^{14}C	5×10^{-3}	2.5×10^{-3}
^{20}O		1.3×10^{-4}

In order to treat the formation of ^{7}Li and ^{11}B with probabilities $S(^7\mathrm{Li}) = S_{^4\mathrm{He}} \times S_{^3\mathrm{H}}$ and $S(^{11}\mathrm{B}) = (S_{^4\mathrm{He}})^2 \times S_{^3\mathrm{H}}$, respectively, we should estimate $S_{^3\mathrm{H}}$. Since our cluster model is one dimensional in η_Z (at average η), we cannot calculate with it the fluctuations in mass asymmetry and, thus, $S_{^3\mathrm{H}}$. For this purpose, we use the statistical approach with the Boltzmann-type formula. The potential energy of the dinuclear system $^4\mathrm{He} + ^{142}\mathrm{Xe}$ is about 3 MeV smaller than the potential energy of the configuration $^3\mathrm{H} + ^{143}\mathrm{Cs}$. Therefore, we obtain $S_{^3\mathrm{H}} = 4.2 \times 10^{-3}$ at the considered excitation energy. The use of the statistical treatment is justified. For example, the formation of ^{6}He needs also more energy than the formation of ^{4}He and the calculated formation probability of ^{6}He from ^{146}Ba is about 31 times smaller than the formation probability of ^{4}He if the statistical approach is used, while the experiments [1] give us 27 times difference.

Since the calculated probabilities $S(^{A_3}Z_3)$ of formation of LCP $^{A_3}Z_3$ are well correlated with the experimental data on the relative yields of ternary fission (table 3), one can conclude that the probability of ternary decay weakly depends on the kind of LCP. Thus, the ratios of the yields of different LCP are ruled by the formation probabilities S of these LCP. With the suggested mechanism of the formation of the LCP one can explain the observed weak dependence of the LCP formation probability S on the excitation energy of the fissioning nucleus [12,8]. While $S_{^4\mathrm{He}}$ weakly depends on E^* at $E^* > 8$ MeV, the spectroscopic factors $S_{^{10}\mathrm{Be}}$ and $S_{^{14}\mathrm{C}}$ show a visible dependence on the excitation (fig. 4). Therefore, the sequential formation of the LCP from the correlated ^{4}He in the region between two heavy fragments looks realistically.

2.4 Neutron multiplicity distribution in binary and ternary fission

The system at scission has the intrinsic excitation energy E^* which can be calculated with eq. (2). In the case of binary fission this energy is assumed to be divided between the fragments proportional to their level densities. Since the fragments are deformed at scission, the relaxation of the deformations to the ground-state deformations takes place after the decay and the energies E_i^{def} of deformations are transformed into the fragment intrinsic excita-

tion energies E_i^*:

$$E_i^* = E^* \frac{a_i}{a_1 + a_2} + E_i^{def}, \tag{11}$$

where a_1 and a_2 are the level density parameters of the nuclei.

For ternary systems, the excitation energy of the LCP is assumed to be small. To overcome the Coulomb barrier, in the considered scission configurations the LCP obtains the energy E^{LCP}. Therefore, the intrinsic excitation energy of the primary fragment ($i = 1$ or 2) of the ternary fission is

$$E_i^* = (E^* - E^{LCP}) \frac{a_i}{a_1 + a_2} + E_i^{def}. \tag{12}$$

Here, we use eq. (2) to calculate E^*. In comparison with the binary fission, the excitation energies of the fragments in the ternary fission is reduced by $E^{LCP} a_i/(a_1 + a_2)$ and smaller E_i^{def}. However, E^* can be larger in ternary fission than in the binary one, like in ^{252}Cf, and the difference of E_i^* in binary and ternary fission can be relatively small.

Due to the excitation energy, the fission fragment can evaporate several neutrons after fission. To calculate the neutron multiplicity distribution, we use the following expression:

$$\langle \nu_i \rangle = \frac{E_i^*}{B_{n_i} + 2T_i}, \tag{13}$$

where B_{n_i} is the energy of separation of the neutron and T_i is the temperature of the fragment, $T_i = (E_i^*/a_i)^{1/2}$. For small excitation energies, we take B_{n_i} as the separation energy of the first neutron. In the case of high excitations we take B_{n_i} as the average over the first and second neutrons. The term $2T_i$ is included to describe the kinetic energy of the evaporated neutron [26].

3 Results and discussions

3.1 Spontaneous ternary fission of ^{252}Cf

3.1.1 Fine structure of TKE-mass distribution

There are several minima of the potential energy of the system as a function of β_1 and β_2 for fixed A_1 and A_2. If we consider the potential energy of the system at scission as a function of A_1, β_1 and β_2, the potential energy surface depends on three coordinates. The deformations β_1 and β_2 of the fragments at the minima have almost the same values for neighboring A_1. Therefore, in the three-dimensional space (β_1, β_2, A_1) the minima of the potential energy with respect to β_1 and β_2 are situated along several lines almost perpendicular to the plane (β_1, β_2). Since the deformations corresponding to minima are energetically preferable, the yields are enhanced for the deformations corresponding to these lines. These enhanced yields are along lines on the TKE-mass distribution which produce fine structures in the TKE-mass distribution. Since the considered potential minima are quite shallow, the produced structures are called fine structures like in the case of binary fission [27]. In our approach we define the TKE of fragments as V_{int} at scission. Since the kinetic energy of the LCP of about 15 MeV at the scission configuration considered, V_{int} almost coincides with the TKE of heavy fragments. In addition, the interaction of the LCP with heavy fragments at scission is quite small because of the mutual compensation of the Coulomb and nuclear forces.

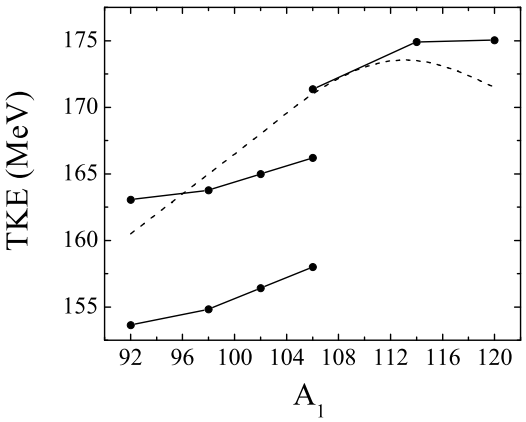

Fig. 5. Predicted fine structure of the TKE-mass distribution for the spontaneous ternary ^{4}He-accompanied fission of ^{252}Cf. The experimental dependence of the mean TKE on A_1 is taken from ref. [28] and presented by the dashed line.

For the binary fission, the calculated structures [14] correlate well with the experimentally found fine structures [27]. These fine structures are different from those produced by the odd-even effect. Indeed, the method for analyzing the fine structure in the experimental data is based on the specific subtraction of a smooth distribution from the measured one [27]. In comparison to the binary fission, the values of β_1 and β_2 in the minima of the ternary systems are smaller and the number of the minima is in general smaller as well. Therefore, the calculated fine structure in fig. 5 for the α-accompanied spontaneous ternary fission of ^{252}Cf is poor and consists only of three lines connecting the points corresponding to the potential minima with respect to β_1 and β_2. For $A_1 = 106$, there are three potential minima (fig. 3) corresponding to different values of β_2 at fixed β_1. For $A_1 < 106$, there are only two potential minima. For $A_1 > 106$, the potential energy as a function of β_1 and β_2 has only one minimum. The upper line in fig. 5 corresponds to the deepest potential minima. For $A_1 = 106$, the energy at the minimum related to this line is 0.2 MeV (1 MeV) smaller than the energy at the minimum related to the middle (lowest) line. The dashed line in fig. 5 shows the experimental dependence of the average TKE of heavy fragments on A_1 taken from ref. [28]. This dashed line is closed to the upper solid line for $A_1 \geq 106$. The products with $A_1 \leq 102$ have the maximal yields at TKE corresponding to the middle line. The fine structure indicated by the lowest solid line in fig. 5 is out of the region of the maximal yields of the fission fragments and can be tried to be found in the experimental data if the fissioning ternary system reaches so large deformations. There are also fine structures in the TKE-

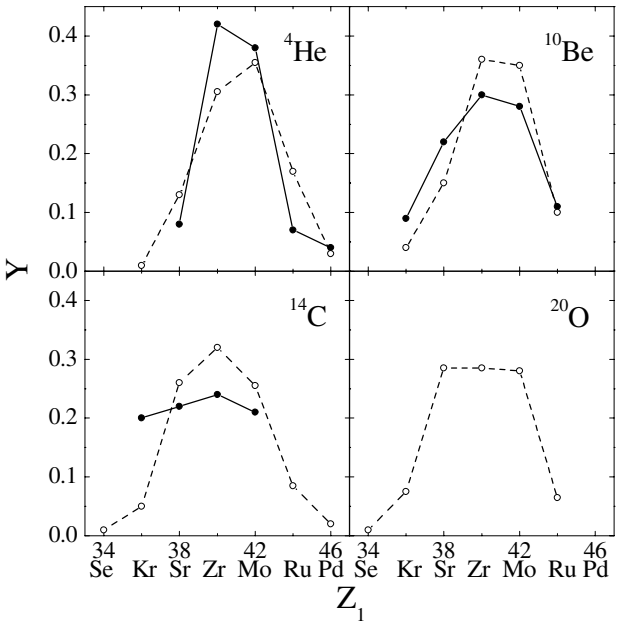

Fig. 6. Charge distributions in the spontaneous ternary fission of ^{252}Cf with different indicated LCP. The calculated and experimental points are shown by open and closed circles, respectively, connected by straight lines.

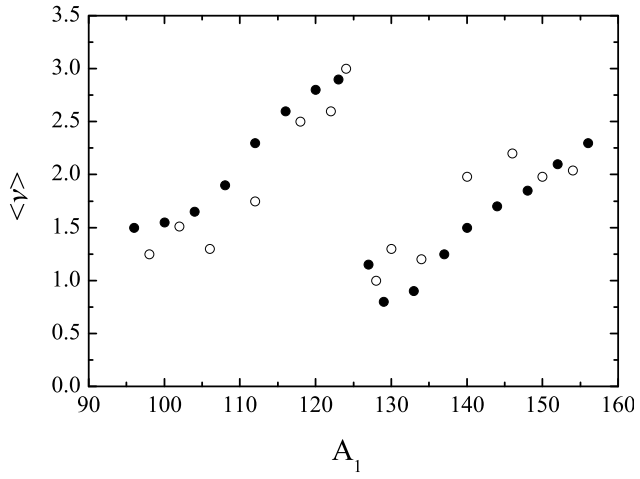

Fig. 7. Neutron multiplicity from individual fragments in the spontaneous binary fission of ^{252}Cf as a function of the fragment mass. The experimental data [1] and calculated results are presented by closed and open circles, respectively.

mass distribution in the case of ternary fission of ^{252}Cf with other LCP. This phenomenon can be observed in the spontaneous and induced ternary fission of actinides and transactinides.

3.1.2 Charge distributions

Let us consider ternary systems formed from the binary ones listed in table 1. The charge distributions related to heavy fragments are calculated with eqs. (5)–(7). The results of our calculations for ^{252}Cf in comparison with the experimental data are shown in fig. 6. Since the binary system Mo + Ba has the largest yield and the potential energy of the ternary system Mo + ^{4}He + Xe is smaller than for Zr + ^{4}He + Ba, the ternary charge distribution with the LCP ^{4}He has a maximum at Mo. This is in agreement with the data of ref. [29], where $Y(\mathrm{Mo} + {}^4\mathrm{He} + \mathrm{Xe})/Y(\mathrm{Zr} + {}^4\mathrm{He} + \mathrm{Ba}) = 1.6$. However, in the recent processing of the experimental data [2] ^{4}He seems to be extracted with a larger preference from the light fragment and the distribution has a maximum at Zr. The width of the distribution seems to be well reproduced in our calculations.

For the LCP ^{10}Be, the maxima of the experimental and calculated distributions coincide. It should be mentioned that the distribution has a larger width than in the case of ^{4}He. For the ^{14}C accompanied ternary fission, again we have a coincidence of the calculated and experimental maxima, but the calculated yield at $Z_1 = 36$ is smaller than in the experiment. The width of the distribution is larger than in the case of ^{10}Be-accompanied ternary fission. In fig. 6 we also predict the charge distribution for ternary fission with the LCP ^{20}O. The tendency of the increase of the width of charge distribution with the charge of LCP can be easily explained. If the LCP is heavier and consists of several α-particles, then from one binary system one can construct more ternary systems with different charge asymmetries.

3.1.3 Neutron multiplicity distribution from each heavy fragment

As a first step, we treat the neutron emission in the binary fission. The calculated neutron multiplicity from individual fragments in the binary fission of ^{252}Cf is compared with the experimental data in fig. 7. Since the mean kinetic energies of the fission fragments are well described with the approach presented [14], the calculated excitation energies of the fragments as well as the neutron multiplicities are in good agreement with the experiment [1].

In α-accompanied ternary fission, the TKE of the heavy fragments, which is equal to the interaction energy V_{int} at scission, is in good agreement with the experimental values in fig. 5. The α-particle obtains a kinetic energy E^{LCP} of about 16 MeV [1] to overcome the Coulomb barrier. The calculated neutron multiplicity from the individual fragments in the spontaneous α-accompanied ternary fission of ^{252}Cf is compared with the experiment [1] in fig. 8. The presented result of calculations with E_1^* and E_2^* (see eq. (10)) has not so good agreement with the experiment as with $E_1^* \to E_1^* - 2$ MeV and $E_2^* \to E_2^* + 2$ MeV but is still satisfactory.

For the ^{10}Be-accompanied fission, the mean kinetic energy of ^{10}Be is about 18 MeV [1,2,30]. However, the neutron multiplicities were measured in ref. [1] with the low-energy cut-off for ^{10}Be which was 26 MeV. Note that for ^{4}He the cut-off is smaller than the mean kinetic energy of ^{4}He. Therefore, for comparison with the data [1] we take $E^{LCP} = 26$ MeV and deal with the data on neutron

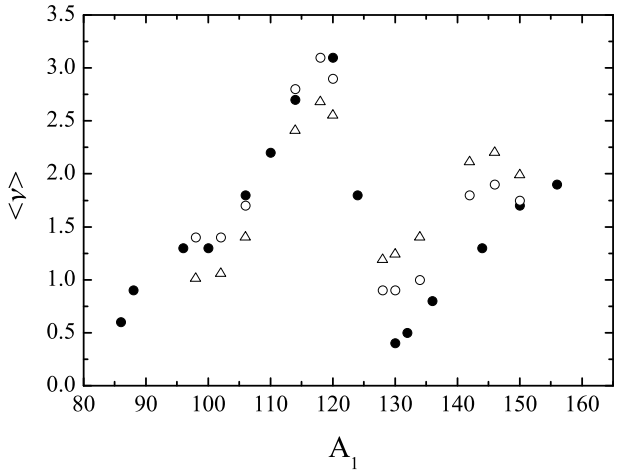

Fig. 8. Neutron multiplicity from the individual fragments in the ^{4}He-accompanied spontaneous ternary fission of ^{252}Cf as a function of the fragment mass. The experimental data [1] are shown by closed circles. The results calculated with excitation energies E_1^* and E_2^* from eq. (10), and with $E_1^* \to E_1^* - 2\,\mathrm{MeV}$ and $E_2^* \to E_2^* + 2\,\mathrm{MeV}$ are presented by open triangles and circles, respectively.

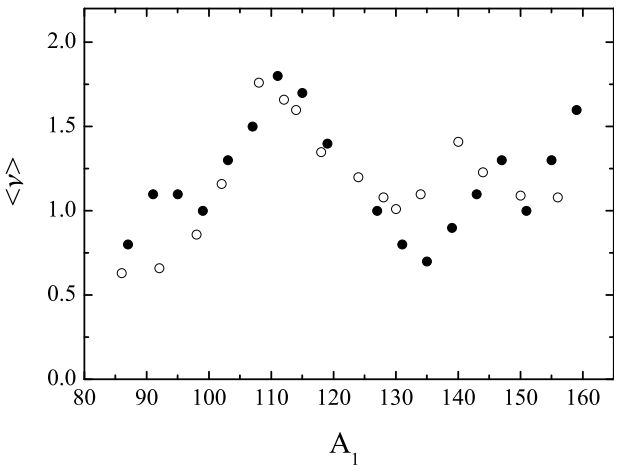

Fig. 9. Neutron multiplicity from the individual fragments in the ^{10}Be-accompanied spontaneous ternary fission of ^{252}Cf as a function of the fragment mass. The experimental data [1] and calculated results with E_i^* $(i = 1, 2)$ from eq. (10) are presented by closed and open circles, respectively.

multiplicity only for a part of the ^{10}Be-accompanied fission. We use E_i^* $(i = 1, 2)$ from eq. (10) in calculations. The comparison of our calculations with the experiment is presented in fig. 9. As in binary fission, the dependence of $\nu(A_1)$ in ternary fission looks like a "sawtooth" curve. For ^{4}He and ^{10}Be as the LCP, the values of $\nu(A_1)$ are almost the same in the vicinity of $A_1 = 132$, indicating the importance of the shell structure at $Z = 50$ and $N = 82$. Our model also predicts the same "sawtooth" curves for the heavier LCP. Quite a good description of neutron multiplicities comes from the possibility of our approach to determine the excitation energies of the fission fragments, as well as their kinetic energy. Indeed, in

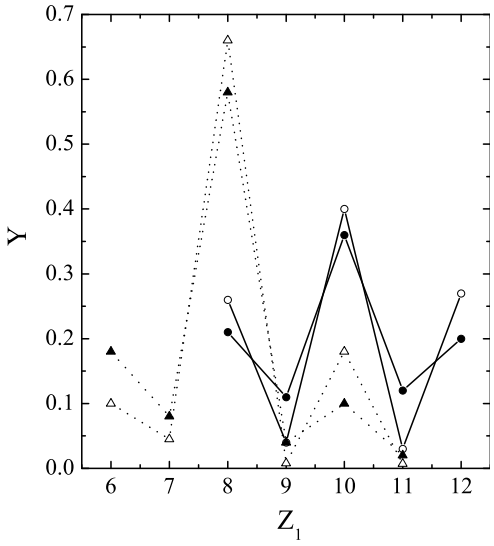

Fig. 10. The calculated (open symbols) and preliminary experimental (closed symbols) [7] charge distributions in the induced ternary fission of ^{56}Ni with the middle particle ^{8}Be (circles) and ^{12}C (triangles).

the scission of the ternary system ^{102}Zr + ^{10}Be + ^{140}Xe we find $V_{int} = 160\,\mathrm{MeV}$ which is in a good agreement with the experimental TKE [1].

3.2 Induced ternary fission of ^{56}Ni

In comparison with ^{252}Cf, ^{56}Ni produced in the reaction ^{32}S + ^{24}Mg [7] has a large angular momentum up to $\sim 45\hbar$ and an excitation energy of about 84 MeV. The deformations of the fragments produced from ^{56}Ni do not practically deviate from their values in the ground states due to the small values of the Coulomb interaction and large stiffness of the light nuclei. Hence the variation in deformation is not necessary and the calculations are performed for the experimental ground-state deformations. There is one peculiarity related to the ^{12}C nucleus as the third particle. The ternary coaxial system with an oblate ^{12}C in the middle is very compact and energetically preferable in the minimum of the interaction potential due to the nuclear part of the interaction, but the barrier for the decay of this configuration is very high. If the ^{12}C fragment in the middle is turned by an angle of 90° around the axis which is perpendicular to the line connecting the centers of heavy fragments, the moment of inertia of the ternary system increases and the energy at the barrier decreases by about 4 MeV at $L = 35$. The decay of the ternary systems with smaller barriers seems to be preferable. The charge distributions for the fission of ^{56}Ni are calculated in the same way like for ^{252}Cf by using eq. (7). In ^{56}Ni we deal with α-particle excited nuclei where $S_{^4\mathrm{He}}$ seems to be close to unity. For ^{56}Ni, the potential energies of the ternary systems at the barriers are larger than the potential energies of the binary systems at the barriers. With increasing angular momentum this difference decreases. However, at $L = 35$ it is still 6–8 MeV that is in agreement with the calculations presented in ref. [3]. Thus, the formation of

a ternary system from the binary one in ^{56}Ni needs the energy taken from the internal excitation energy.

Figure 10 demonstrates a good agreement of the charge distributions with the available preliminary data [7] for the ternary fission of ^{56}Ni accompanied by ^{8}Be and ^{12}C as the third particles. The calculations are performed at $L = 35$ because the higher partial waves mostly contribute to the cross-section. The structures of the charge distributions are well reproduced. The difference of the potential energies of the ternary systems with ^{8}Be and ^{12}C at the barriers weakly depends on L and is within 1–2 MeV. Therefore, the yields of ternary decays with ^{8}Be and ^{12}C are close to each other. One cannot compare the charge distribution for ternary fission with ^{4}He as the third particle with the experiment because the binary fission with sequential evaporation of ^{4}He from one of the excited fragments cannot be distinguished from the ternary fission events.

4 Summary

We developed the model of ternary fission based on potential energy calculations of ternary systems at scission and on statistical analysis. The used cluster description of scission configurations is convenient to include a variation of the fragment deformations, and allows us also to vary the charges and masses of the fragments separately and to consider all possible scission configurations. The excitation energy of the fissioning system at scission is consistently calculated in our model as well as the kinetic energy of the fragments after fission. The formation of the ternary system was considered as the second step after the formation of the binary system by means of extracting one or several α-particles and neutrons from one or both binary fragments in the region of their interaction.

Using the model developed, we described the charge distributions for the fission of the heavy nucleus ^{252}Cf and the light nucleus ^{56}Ni accompanied by various LCP. The relative yields of different LCP and mean TKE of fragments are calculated for the fission of ^{252}Cf and are in good agreement with the experimental results. Based on the calculations of the excitation energy at scission we obtained a good agreement with the experimental data on neutron multiplicity distributions for the binary and ternary fission of ^{252}Cf. The success in the description of the ternary fission of both heavy and light nuclei allows us to conclude on the validity of our approach which can be improved by including dynamical effects in the future. The future experimental observations of the predicted fine structures of the TKE-mass distribution, analogously to those observed in the binary fission, and the charge distribution for the ^{20}O-accompanied ternary fission will additionally justify our approach.

We thank Professors W. von Oertzen and Yu.V. Pyatkov, and Dr D.V. Kamanin for fruitful discussions and suggestions. This work was supported by DFG (Bonn), RFBR (Moscow) and Volkswagen-Stiftung (Hannover).

References

1. M. Mutterer *et al.*, in *Proceedings of the 3rd International Conference on Dynamical Aspects of Nuclear Fission, Casta-Papiernicka, Slovak Republic*, edited by J. Kliman, B.I. Pustylnik (JINR, Dubna, 1996) p. 250 and references therein; M. Mutterer *et al.*, Nucl. Phys. A **738**, 122 (2004).
2. G.M. Ter-Akopian *et al.*, Phys. At. Nuclei **67**, 1860 (2004).
3. A.V. Ramayya *et al.*, Rhys. Rev. C **57**, 2370 (1998).
4. J.H. Hamilton *et al.*, Prog. Part. Nucl. Phys. **38**, 273 (1997).
5. I.D. Alkhazov, B.F. Gerasimenko, A.V. Kuznetsov, B.F. Petrov, V.A. Rubchenya, V.I. Shpakov, Sov. J. Nucl. Phys. **57**, 978 (1988).
6. S. Oberstedt *et al.*, Nucl. Phys. A **761**, 173 (2005).
7. W. von Oertzen *et al.*, Preprint IReS-05-17 (2005).
8. I. Halpern, Annu. Rev. Nucl. Sci. **21**, 245 (1971).
9. N. Carjan, A. Sandulescu, V.V. Pashkevich, Phys. Rev. C **11**, 782 (1975).
10. G.A. Pik-Pichak, Sov. J. Nucl. Phys. **40**, 215 (1984).
11. A.S. Roshchin, V.A. Rubchenya, S.G. Yavshits, Sov. J. Nucl. Phys. **53**, 909 (1991).
12. V.A. Rubchenya, S.G. Yavshits, Z. Phys. A **329**, 217 (1988).
13. D.S. Delion, A. Florescu, A. Sandulescu, Phys. Rev. C **63**, 044312 (2001); A. Sandulescu *et al.*, J. Phys. G. **24**, 181 (1996).
14. A.V. Andreev, G.G. Adamian, N.V. Antonenko, S.P. Ivanova, W. Scheid, Eur. Phys. J. A **22**, 51 (2004).
15. J. Maruhn, W. Greiner, Z. Phys. **251**, 431 (1972).
16. G.G. Adamian *et al.*, Int. J. Mod. Phys. E **5**, 191 (1996).
17. T.M. Shneidman, G.G. Adamian, N.V. Antonenko, R.V. Jolos, W. Scheid, Phys. Lett. B **526**, 322 (2002).
18. M. Wöstheinrich, M. Hesse, F. Gönnenwein, in *Proceedings of the 3rd International Conference on Dynamical Aspects of Nuclear Fission, Casta-Papiernicka, Slovak Republic*, edited by J. Kliman, B.I. Pustylnik (JINR, Dubna, 1996) p. 231.
19. A.V. Ignatyuk, *Statistical Properties of Excited Atomic Nuclei* (Energoatomizdat, Moscow, 1983).
20. S.N. Kuklin, G.G. Adamian, N.V. Antonenko, Phys. Rev. C **71**, 014301 (2005).
21. J.K. Tuli, *Nuclear Wallet Cards* (BNL, New York, 2000).
22. P. Moeller, J.R. Nix, At. Data Nucl. Data Tables **39**, 213 (1988).
23. S. Raman *et al.*, At. Data Nucl. Data Tables **78**, 1 (2001).
24. Y.S. Zamyatnin *et al.*, Sov. J. Part. Nuclei **21**, 537 (1990).
25. S.N. Kuklin *et al.*, to be published in Phys. At. Nuclei.
26. E.A. Cherepanov, A.S. Iljinov, Nucleonika **25**, 611 (1980).
27. Yu.V. Pyatkov, V.G. Tishchenko, V.V. Pashkevich, V.A. Maslov, D.V. Kamanin, I.V. Kljuev, W.H. Trzaska, Nucl. Instrum. Methods A **488**, 381 (2002).
28. P. Fong, Phys. Rev. C **2**, 735 (1970).
29. M. Jandel *et al.*, in *Proceedings of the International Conference on Fission and Properties of Neutron-Rich Nuclei, Sanibel Island, Florida, 2002*, edited by J.H. Hamilton, A.V. Ramayya, H.K. Carter (World Scientific, Singapore, 2003) p. 448.
30. A.A. Vorobjev, V.T. Grachev, I.A. Kondurov, A.M. Nikitin, D.M. Seliverstov, Phys. Part. Nucl. **2**, 941 (1972).